Available online at www.sciencedirect.com

ScienceDirect

Energy Procedia 51 (2014) 85 – 98

Energy Procedia

7th Trondheim CCS Conference, TCCS-7, June 5-6 2013, Trondheim, Norway

$(Fe_{1-x}Mn_x)Ti_yO_3$ based oxygen carriers for chemical-looping combustion and chemical-looping with oxygen uncoupling

Magnus Rydén[a,*], Malin Källén[a], Dazheng Jing[b], Ali Hedayati[a], Tobias Mattisson[a], Anders Lyngfelt[a]

[a]*Department of Energy and Environment, Chalmers University of Technology, Göteborg, Sweden*

[b]*Department of Environmental Inorganic Chemistry, Chalmers University of Technology, Göteborg, Sweden*

Abstract

The manganese based ilmenite analogue pyrophanite ($MnTiO_3$) and six other combined $(Fe1_{-x}Mn_x)Ti_yO_3$ oxides have been examined as oxygen-carrier materials for chemical-looping combustion (CLC) and chemical-looping with oxygen uncoupling (CLOU). Particles with different compositions were manufactured by spray drying and studied by consecutive reduction and oxidation at 850-1050°C in a batch fluidized-bed reactor using CH_4 as fuel. A fuel conversion of 80-99% could be achieved with most materials, with different formulations being favored at different temperature levels. The exception was pure $MnTiO_3$ which had very limited reactivity with CH_4. The oxygen uncoupling behavior was examined by exposing the oxygen-carrier particles to an inert atmosphere of N_2. The apparent equilibrium concentration during fluidization with pure N_2 ranged from zero to 0.9% O_2, depending on temperature and particle composition. One material $(Fe_{0.50}Mn_{0.50})TiO_3$ was selected and further examined by 12 h of experiments in a small continuously operating circulating fluidized-bed reactor. Up to 80% conversion of natural gas was achieved at 910°C, but defluidization occurred when the temperature was increased to 950°C.

Selection and peer-review under responsibility of SINTEF Energi AS

Keywords: Carbon capture; Chemical-looping combustion; Chemical-looping with oxygen uncoupling; Pyrophanite; Ilmenite

* Corresponding author. Tel.: +46-31-7721457
E-mail address: magnus.ryden@chalmers.se

Selection and peer-review under responsibility of SINTEF Energi AS
doi:10.1016/j.egypro.2014.07.010

1. Introduction

This paper describes an experimental study examining the possibility to use combined manganese-iron-titania oxides as oxygen carriers for chemical-looping combustion (CLC) and chemical-looping with oxygen uncoupling (CLOU). These are innovate processes for capturing CO_2 during oxidation of hydrocarbon fuels. The ultimate goal with this research effort is to contribute to the development of efficient methods to reduce the emissions of the greenhouse gas CO_2 to the atmosphere during utilization of such fuels. A thorough description of how so called carbon capture and storage (CCS) can contribute to reduced emissions of the greenhouse gas CO_2 to the atmosphere can be found, for example in IPCC's special report about the topic[1].

2. Background

2.1. Chemical-looping combustion

Chemical-looping combustion (CLC) is a method for combustion of fuels in which the fuel is oxidized in two separate reactor vessels, one air reactor (AR) and one fuel reactor (FR). A solid oxygen-carrier (MeO_x) performs the task of transporting oxygen to the fuel and circulates continuously between the two reactors. In the fuel reactor, it is reduced by the fuel, which in turn is oxidized to CO_2 and H_2O according to reaction (1). In the air reactor, it is oxidized to its initial state with O_2 from the air according to reaction (2). The sum of reactions for the reactor system as a whole is complete combustion of the fuel with O_2, reaction (3), and the net energy released is the same as in ordinary combustion.

$$C_nH_m(g) + (2n+½m)MeO_x(s) \rightarrow nCO_2(g) + (½m)H_2O(g) + (2n+½m)MeO_{x-1}(s) \quad (1)$$

$$MeO_{x-1}(s) + ½O_2(g) \rightarrow MeO_x(s) \quad (2)$$

$$C_nH_m(g) + (n+¼m)O_2(g) \rightarrow nCO_2(g) + (½m)H_2O(g) \quad (3)$$

The expected operating temperature is in the range of 850-1050°C. A feasible design would be to utilize fluidized beds arranged in similar fashion as in a circulating fluidized-bed boiler (CFB), with the difference that the inert bed material used in such facilities would be replaced with an active oxygen-carrier material. A schematic description of chemical-looping combustion can be found in Figure 1.

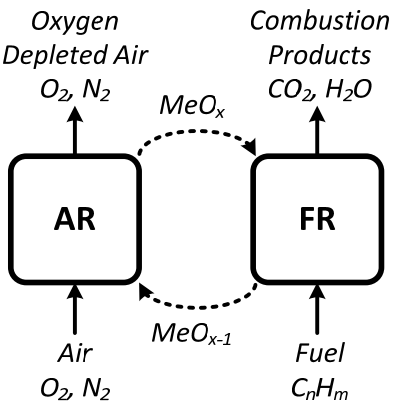

Fig. 1. *Schematic description of chemical-looping combustion.*

The general ideas behind chemical-looping combustion can be traced back to the middle of the past century to work by Lewis and Gilliland[2]. Other early work includes a study by Richter and Knoche[3], who suggested a fuel oxidation reaction scheme involving two intermediate reactions with a metal oxide as oxygen carrier in order to reduce irreversibility compared to ordinary combustion. Ishida et al.[4] came up with the name chemical-looping combustion in 1987. A practicable design of a chemical-looping combustor arranged as a circulating fluidized-bed reactor was suggested by Lyngfelt et al.[5] in 2001.

Some oxygen-carrier materials are capable of releasing gas-phase O_2 directly in the fuel reactor according to reaction (4).

$$MeO_x(s) \leftrightarrow MeO_{1-x}(s) + \tfrac{1}{2}O_2(g) \quad (4)$$

In principle, O_2 will be released until thermodynamic equilibrium for reaction (4) is obtained. If there is a fuel present in the fuel reactor it will react directly with released O_2 according to reaction (3), which will facilitate further O_2 release until all available fuel is consumed. The reduced oxygen carrier can then be recirculated to the air reactor where it is reoxidized according to reaction (2).

This alternative reaction scheme is referred to as chemical-looping with oxygen uncoupling (CLOU), see Mattisson et al.[6]. Here the mechanism by which the fuel is oxidized is different. In ordinary chemical-looping combustion, the oxidation of fuel takes place mainly via gas-solids reactions gas solids reactions (between the gaseous fuel and solid oxygen carrier). So if the fuel is a solid (coal, coke, biochar etc) it has to be gasified in order to be able to react with the oxygen carrier. In contrast, in chemical-looping with oxygen uncoupling the oxidation of the fuel can proceed by direct combustion. Leion et al.[7] have shown that oxidation of solid fuels can be much faster using this reaction scheme, compared to conventional chemical-looping combustion that relies on char gasification.

Both chemical-looping combustion and chemical-looping with oxygen uncoupling provides some intriguing opportunities. Most importantly, fuel is not mixed with N_2 from the combustion air. Hence cooling of the flue gas and condensation of the steam produced in the fuel reactor is sufficient to obtain almost pure CO_2. There is no inherent energy penalty or cost associated with chemical-looping combustion, so oxidation of carbon-containing fuels with this method would be an ideal technology for carbon capture and storage. A comprehensive review of chemical-looping combustion has recently been provided by Adánez et al.[8], while materials for chemical-looping with oxygen uncoupling has been reviewed by Mattisson [9].

2.2. Combined oxides of manganese, iron and titanium oxides as oxygen carrier

The most commonly proposed oxygen-carrier materials for chemical-looping applications are synthetic particles of monometallic oxides based on Fe_2O_3, NiO, CuO and Mn_3O_4. Such active phases can be used as is, or in composite particles together with inert support materials such as for example Al_2O_3, $MgAl_2O_3$ or ZrO_2, see Adanez et al.[8] for a comprehensive review.

Another option would be to use minerals or ores as oxygen carrier, which could be cheaper. One of the most extensively examined such material is ilmenite which is a common mineral with the chemical composition $FeTiO_3$. The term ilmenite is also used for various iron-titanium ores rich with $FeTiO_3$ and its oxidized counterpart psuedobrookite, Fe_2TiO_5. It is cheap, nontoxic, and the most abundant of all titanium minerals and has proven to be an attractive oxygen-carrier material. During chemical-looping combustion, the fully reduced state would be $FeTiO_3$, corresponding to $FeO+TiO_2$, while the fully oxidized level would be $Fe_2TiO_5+TiO_2$, corresponding to $Fe_2O_3+2TiO_2$. Ilmenite has been examined as oxygen-carrier material for chemical-looping combustion by several research groups using a wide range of reactors, fuels and operational conditions[10-22].

A detailed review of the thermodynamics involved in the use of ilmenite as oxygen carrier for chemical looping combustion have been presented by Luckos and den Hoed[23]. It is clear that from a thermodynamic point of view,

ilmenite should not be capable of releasing any gas phase O_2 during temperature levels typically used for chemical-looping combustion experiments, i.e. below 1050°C. In some experiments very minor O_2 release have been observed but this is likely an effect of impurities in the ilmenite, see Rydén et al.[24]. Pure ilmenite should not be capable of providing gaseous O_2 via reaction (4), which is a pity since the mechanical properties of ilmenite are considered as quite adequate.

Substituting iron with manganese in ilmenite yields pyrophanite ($MnTiO_3$), a mineral that like ilmenite is of trigonal rhombohedral crystal structure. It can be assumed that manganese and iron should be interchangeable within this structure, forming ilmentite-pyrophanite solid solutions. Substituting iron for manganese in the ilmenite structure could be expected to increase the propensity for O_2 release in gas phase, thus obtaining an oxygen carrier suitable for chemical-looping with oxygen uncoupling.

It has previously been experimentally verified that Fe_2O_3-Mn_2O_3 solid solutions exhibit vastly superior O_2 uncoupling characteristics compared to its monometallic counterparts, see Azimi et al.[25,26]. The apparent reason is the possibility to alter the temperature of O_2 uncoupling from hausmannite $(Mn_xFe_{1-x})O_3$ by altering the manganese and iron content of the solid solution, see Rydén et al.[27]. Unfortunately, Fe_2O_3-Mn_2O_3 solid solutions have exhibited poor durability in continuous operation, see Rydén et al.[28].

2.3. The aim of this study

This study reports the examination of pyrophanite ($MnTiO_3$) and six different combined $(Fe1_{-x}Mn_x)Ti_yO_3$ oxides as oxygen-carrier materials. The aim is to show that ilmentite-pyrophanite solid solutions are capable of releasing gas phase O_2 at conditions relevant for chemical-looping applications, while hopefully retaining mechanical properties similar to ilmenite.

3. Experimental

3.1. Manufacturing of oxygen-carrier materials

All oxygen-carriers particles examined in this study were manufactured by VITO in Belgium by spray drying. The general procedure was as follows. Powder mixtures of the raw materials were dispersed in deionized water containing organic additives, organic binder and dispersants. The water-based suspension was continuously stirred with a propeller blade mixer while being pumped to a 2-fluid nozzle, positioned in the lower cone part of the spray-drier. Obtained particles were sieved, and the fraction within the desired size range was separated from the rest of the spray-dried product. Sieved particles were then calcined in air at 1100°C for 4 h. After calcination, the particles were sieved once more so that all particles used for experimental evaluation would be of well-defined size.

A summary of manufactured materials and their physical properties can be found in Table 1. The bulk density was measured for particles in the size range of 125-180 µm using a graduated cylinder. The reported crushing strength is the average force required to fracture a single particle, as measured with a digital force gauge on particles in the size range of 180-250 µm.

Table 1. Summary of oxygen-carriers materials examined in this study.

Sample	Molar composition	Bulk density (kg/m^3)	Crushing strength (N)
F17MT51	$(Fe_{0.33}Mn_{0.67})TiO_x$	1430	0.7
F25MT51	$(Fe_{0.50}Mn_{0.50})TiO_x$	1400	0.7
F34MT50	$(Fe_{0.67}Mn_{0.33})TiO_x$	1380	0.8
M49T	$MnTiO_x$	1100	0.7
F31MT9	$(Fe_{0.33}Mn_{0.67})Ti_{0.1}O_x$	1640	0.7
F46MT9	$(Fe_{0.50}Mn_{0.50})Ti_{0.1}O_x$	1380	0.8
F61MT9	$(Fe_{0.67}Mn_{0.33})Ti_{0.1}O_x$	1410	0.9

Aside from pure pyrophanite, the materials can be divided into two main categories, namely ilmenite-pyrophanite analogues (first three materials in Table 1), and combined iron-manganese oxides with minor addition of titania (last three materials).

3.2. Experimental setup for batch experiments

Batch experiments were carried out in an 820 mm long quartz reactor with an inner diameter of 22 mm. A porous quartz plate, on which the sample of oxygen carrier and CO_2 sorbent was applied, was located 370 mm above the bottom. During operation, the sample was fluidized by adding gas to the bottom of the reactor, and the porous plate acted as gas distributor.

The reactor temperature was measured with thermocouples located 5 mm below and 25 mm above the porous plate. The pressure drop over the particle bed was measured with a pressure transducer operating at a frequency of 20 Hz. The pressure drop over a quartz plate is approximately constant for constant flows, so by measuring fluctuations in the pressure drop it was possible to determine if the particle bed was fluidized or not.

At the top of the reactor was a plug of quartz wool, in which elutriated solid fines was captured. The product gas was then subject to cooling and condensation of water at room temperature. After this step, the composition of the dry gas was measured with a gas analyser with three parallel channels. CO_2, CO and CH_4 were measured with an infrared sensor, O_2 was measured with a paramagnetic sensor, and H_2 was measured by a sensor based on thermal conductivity. A schematic description of the experimental setup is shown in Figure 2.

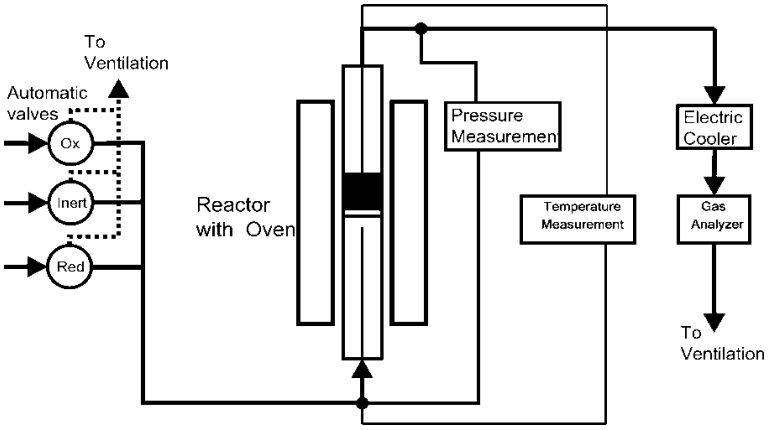

Fig. 2. *Schematic description of the experimental setup used for batch experiments.*

The experimental procedure was as follows. 15 g particle in the size range 125-180 µm was placed on the porous plate. The reactor was then assembled and placed inside an electrically heated furnace. During heat up to 850°C the sample was fluidized with an oxidizing gas mixture in order to ensure full oxidation.

The experiments were initiated by performing a few (1-5 reductions, 30-60 s each) redox cycles using 450 ml/min of a syngas mixture consisting of 50% CO and 50% H_2 at 850°C as fuel. The reason was to ensure that the oxygen carriers were properly reduced and oxidized a few times prior to O_2 uncoupling experiments. Hence the use of syngas, which is perceived as considerably more reactive with oxygen-carrier materials compared to CH_4. The preceding syngas experiments will not be further discussed.

Chemical-looping experiments were then conducted by switching between different fluidization gases according to a scheme described in Table 2.

Table 2. Examination scheme for batch experiments. Each cycle constitutes reduction for a specified time period passively with N_2 or actively with CH_4, followed by oxidation until the sample is fully reoxidized.

Cycle	Temperature (°C)	Reducing gas	Reduction time (s)
1-2	850	Inert (N_2)	360
3-4	850	Fuel (CH_4)	20
3-5	900	Inert (N_2)	360
6-7	900	Fuel (CH_4)	20
8-10	950	Inert (N_2)	360
11-12	950	Fuel (CH_4)	20
13-14	1000	Inert (N_2)	360
15-16	1000	Fuel (CH_4)	20
17-18	1050	Inert (N_2)	360
19-20	1050	Fuel (CH_4)	20
21-22	950	Inert (N_2)	360
23-24	950	Fuel (CH_4)	20

The following gases and gas flows were used:

- Oxidation: 900 ml_n/min with a mixture of 5% O_2 and 95% N_2. To simulate the expected conditions at the top of the air reactor in a future chemical-looping combustion facility.
- Inert: 600 ml/min with 100% N_2. To examine O_2 release via reaction (4) in inert atmosphere, and also to flush the reactor of reactive gases for 60 s in between each fuel and oxidizing period.
- Reduction: 450 ml/min with 100% CH_4. To examine reactivity with natural gas and examine behaviour during deep reduction of each samples.

In this paper, the reactivity of each oxygen carrier with CH_4 is quantified in terms of gas yield, γ_{CH4}, defined as the fraction of CO_2 in dry flue gas divided by the sum of the fractions of carbon containing gases, which when CH_4 is used as fuel constitutes CO_2, CO and CH_4. γ_{CH4} is defined in equation (5), in which y_i is the dry gas concentration (vol. %) of gas component *i*:

$$\gamma_{CH4} = \frac{y_{CO_2}}{y_{CO_2} + y_{CH_4} + y_{CO}} \tag{5}$$

The mass based conversion of the oxygen carrier, ω, is defined as the mass of the sample, m, divided with the mass of the fully oxidized sample, m_{ox}, as is defined in equation (6):

$$\omega = \frac{m}{m_{ox}} \tag{6}$$

The mass based conversion of the oxygen carrier for a specific time period can be calculated by integration over a time interval, as is described in equation (7), in which M_O is the molar mass of oxygen and $\dot{n}_{out}$ is the molar flow out of the reactor. Equation (7) basically describes a species balance over the reactor, and is valid only when CH_4 is used as fuel.

$$\omega_i = \omega_{i-1} - \int_{t_0}^{t_1} \frac{\dot{n}_{out} M_O}{m_{ox}} \left(4 y_{CO_2} + 3 y_{CO} + 2 y_{O_2} - y_{H_2}\right) dt \quad (7)$$

3.3. Experimental setup for continuous operation

The continuous experiments were carried out in a small-scale laboratory reactor made of temperature and deformation resistant stainless steel. The same reactor has previously been used for different kinds of experiments involving liquid fuels[29,30] and hydrogen generation[31]. A schematic description of the reactor is shown in Figure 3.

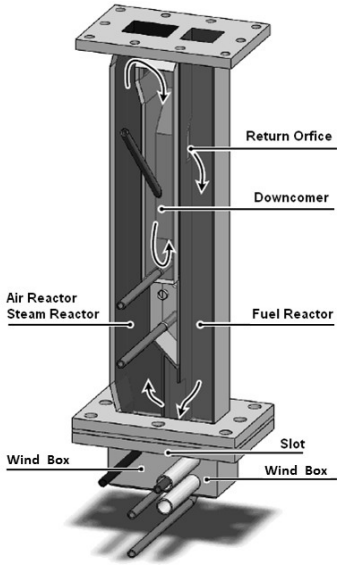

Fig. 3. *Schematic description of the two-compartment fluidized-bed reactor.*

The reactor is 300 mm high. The fuel reactor measures 25 mm × 25 mm. The base of the air reactor is 25 mm × 42 mm, while the upper narrow part is 25 mm × 25 mm. Fuel and air enter the system through separate wind boxes, located in the bottom of the reactor. Porous quartz plates act as gas distributors. For the experiments presented in this paper, 250 g of particles in the size range 90-212 μm were added to the reactor. This corresponds to a bed height in the air and fuel reactor of roughly 10 cm, taken into consideration that a considerable share of the particles was located in the downcomer during operation.

In the air reactor the gas velocity is sufficiently high for oxygen-carrier particles to be thrown upwards. Above the reactor there is a particle separation box (not shown in figure 3) in which the cross-section area is increased and gas velocity reduced so that particles fall back into the reactor. A fraction of these particles falls into the downcomer, entering a J-type loop-seal. From the loop-seal, particles overflow into the fuel reactor via the return orifice. The fuel reactor is a bubbling bed. In the bottom particles return to the air reactor through a U-type slot and thus a continuous circulation of oxygen-carrier particles is obtained. The downcomer and the slot are fluidized with small amounts of inert gas such as argon, which is added via thin pipes perforated by holes, rather than through porous plates.

The whole reactor is placed inside an electrically heated furnace. The temperature in each reactor section is measured with thermocouples located inside the particle beds, a few centimetres above each bottom plate. Along the reactor sections there are several pressure-measuring taps. By measuring differential pressures between these spots it is possible to estimate where particles are located in the system, and to detect abnormalities in the fluidization.

For gas analysis, gas flows in the order of 0.50 L_n/min gas is extracted downstream of the air reactor and fuel reactor respectively. Each of these flows passes through separate particle filters, coolers and water traps. CO_2, CO and CH_4 were measured using infrared analysers while O_2 was measured with paramagnetic sensors. Excess gas that was not needed for analysis passed through a textile filter in order to catch elutriated fines and particles, prior to release in a chimney.

4. Results

4.1. O_2 release during fluidization with N_2

All samples were found to release gas phase O_2 during fluidization with N_2, albeit pure pyrophanite (MT51) only at very low level, see Figure 4-5.

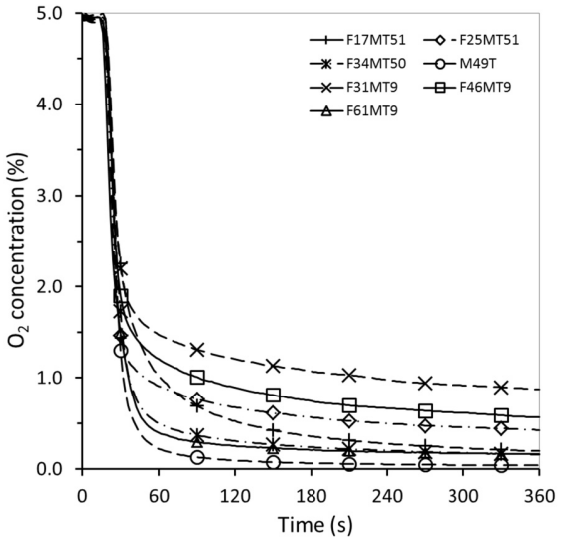

Fig. 4. *O_2 concentration as function of time during fluidization with N_2 at 950°C.*

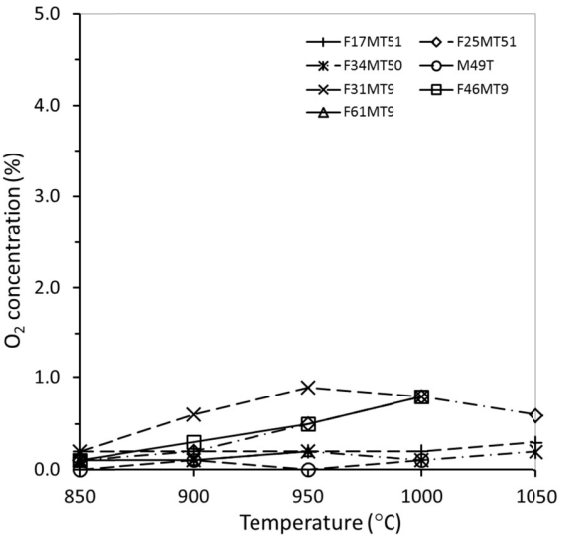

Fig. 5. *O_2 concentration at the end of N_2 period as function of temperature.*

In Figure 4, the fluidization gas is switched from 5% O_2 to 100% N_2 at t=0. There is a slight time delay in the system then the measured outlet concentration of O_2 is rapidly decreased. From this point, measured O_2 is due to O_2 uncoupling from the oxygen carrier so any value above zero verifies that the material could be suitable for chemical-looping with O_2 uncoupling.

In figures 4-5 it can be seen that two materials with only little Ti in the structure (F31MT9, F46MT9) were capable of releasing more O_2 than the ilmenite-pyrophanite analogues at temperatures below 950°C. This is not surprising since iron-manganese oxides by themselves have shown very good O_2 uncoupling properties at these and even lower temperature levels, see Azimi et al.[25,26]. All samples with low Ti content defluidized at temperatures above 1000°C, however. Defluidization means loss of horizontal and vertical mixing of solids in the bed and occurs when the forces holding the particles together becomes larger than the forces providing mixing. It can be seen as loss of pressure drop and pressure fluctuations over the bed. Defluidization due to high temperature is usually attributed to particles becoming sticky as the melting point of one or more of the phases involved are approached.

Samples with higher Ti content did not defluidize. Instead their performance typically improved with temperature. Of those materials F25MT51 clearly had the best O_2 uncoupling properties providing 0.5% already at 950°C. The results of the O_2 uncoupling experiments are summarized in Table 3.

Table 3. O_2 concentration is at the end of the 2nd inert period at each examined temperature. *df* indicates defluidization.

Sample	O_2 850°C (%)	O_2 900°C (%)	O_2 950°C (%)	O_2 1000°C (%)	O_2 1050°C (%)
F17MT51	0.2	0.2	0.2	0.2	0.3
F25MT51	0.1	0.2	0.5	0.8	0.6
F34MT50	0.1	0.1	0.2	0.1	0.2
M49T	0	0.1	0	0.1	*df*
F31MT9	0.2	0.6	0.9	0.8	*df*
F46MT9	0.1	0.3	0.5	0.8	*df*
F61MT9	0.1	0.1	0.2	*df*	*df*

4.2. Experiments with CH_4

The reactivity towards CH_4 at 950°C for the different samples is shown in Figure 6.

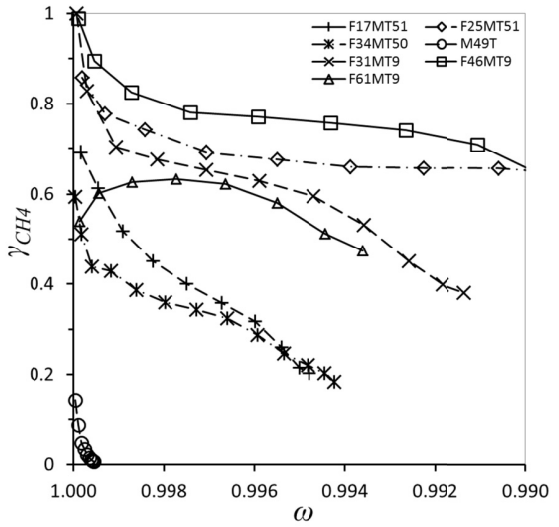

Figure 6. *Gas yield (γ_{CH4}) as a function of solid conversion (ω) for the 2nd methane period at 950°C.*

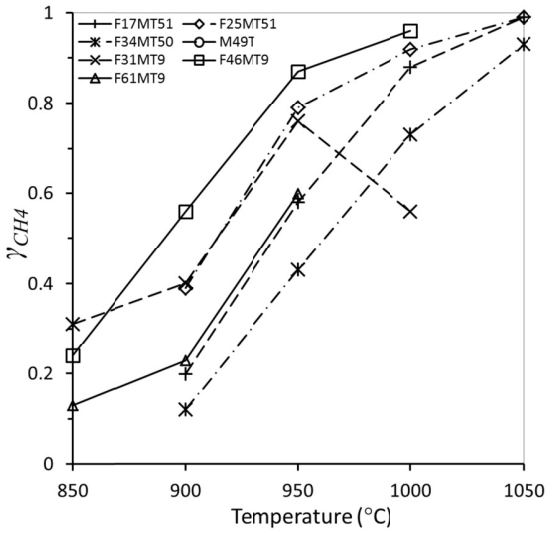

Figure 7. *Average gas yield (γ_{CH4}) for the period ω=1-0.998 as function of temperature.*

In Figure 6 it can be seen that the conversion of fuel to CO_2 (gas yield, γ_{CH4}) initially is higher for all samples, but decrease as the sample is reduced. Pure pyrophanite does barely react with the fuel at all, while the other materials were capable to convert a large fraction of the CH_4 that was added to the reactor CO_2. It is evident that the materials which exhibited highest O_2 release at 950°C also provide the highest fuel conversion at 950°C. Of those two have small Ti content (F31MT9, F46MT9) while one has higher (F25MT51). These materials were capable of converting almost all fuel to CO_2, albeit only when the degree of reduction ω was very high.

In general, the reactivity was low for all materials at 850°C, but increased greatly as function of temperature. This is illustrated in Figure 7, in which the average gas yield (γ_{CH4}) of each sample for the period ω=1-0.998 is shown as function of temperature. Here data for M49T as well as for F34MT50 and F17MT51 at 850°C are missing because reaction rates were so low so that ω=0.998 was not reached within the set time frame. Also some data for samples with low Ti content at 1000°C and above are missing. This is because those samples defluidized at higher temperatures, as has been explained above.

For samples with high Ti content, the reactivity with fuel increased in an almost linear fashion as function of temperature, except for F25MT51 which provided reasonably good reactivity already at 950°C. F31MT9 had lower reactivity at 1000°C than at 950°C. This is consistent with the O_2 release of this material which also was lower at 1000°C, see Table 3. The results of the CH_4 experiments are summarized in Table 4 below.

Table 4. Average gas yield for the period ω=1-0.998 for the 2nd cycle at each temperature. *na* indicates that reduction to ω=0.998 did not happen while *df* indicates defluidization.

Sample	γ_{CH4} 850°C (-)	γ_{CH4} 900°C (-)	γ_{CH4} 950°C (-)	γ_{CH4} 1000°C (-)	γ_{CH4} 1050°C (-)
F17MT51	*na*	0.20	0.58	0.88	0.99
F25MT51	*na*	0.39	0.79	0.92	0.99
F34MT50	*na*	0.12	0.43	0.73	0.93
M49T	*na*	*na*	*na*	*na*	*df*
F31MT9	0.31	0.40	0.76	0.56	*df*
F46MT9	0.24	0.56	0.87	0.96	*df*
F61MT9	0.13	0.23	0.60	*df*	*df*

It shall be pointed out that data in Figure 7 and Table 4 are valid only for the period ω=1-0.998, which means that only 0.2 wt% oxygen has been removed from the particles. Deeper reduction would result in less good fuel conversion, as is illustrated in Figure 6. In this experimental series the particles was reduced at most ≈1.5 wt% which occurred during reduction at 1050°C, when the reactivity was very high.

4.3. Effect of operation at high temperature

Following operation at 1050°C, some additional experiments were performed with N_2 and CH_4 at 950°C (cycle 21-24 in Table 2). This was done in order to examine if the particles were subject to irreversible changes in their properties over the course of the experimental series. The results are summarized in Figures 8-9 below. Data for M49T, F31MT9, F46MT9 and F61MT9 are left out since these samples defluidized at 1000-1050°C.

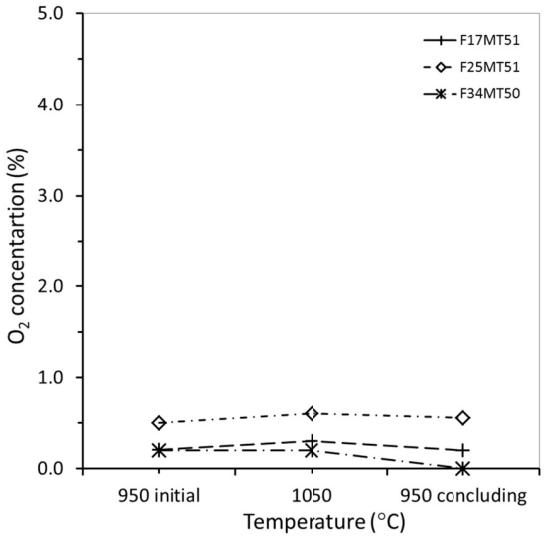

Figure 8. *O_2 concentration at the end of N_2 period for initial 950°C cycle, 1050°C cycle, and concluding 950°C cycle.*

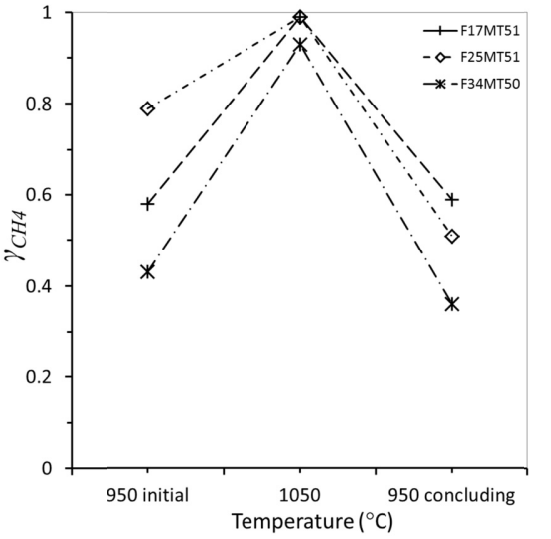

Figure 9. *Average gas yield (γ_{CH4}) for the period ω=1-0.998 for initial 950°C cycle, 1050°C cycle, and concluding 950°C cycle.*

In figures 8-9, it can be seen that F17MT51 maintained its properties well, while F34MT50 exhibited a loss in its O_2 uncoupling ability and F25MT51 experienced a significant reduction in its ability to convert CH_4.

4.4. Experiments in continuously operating reactor

The material F25MT51 showed a combination of good reactivity with CH_4, considerable release of gas phase O_2 already at 950°C and favourable fluidization properties. Because of this it was chosen for further examination by continuous operation in the small-scale laboratory reactor.

The fuel flow was 0.3 L_N/min natural gas, the air flow was 6-8 L_N/min and the temperature in the fuel reactor was 910°C. The amount of oxygen carrier particles added to the reactor was 250 g. The experiments were conducted during three days and the total time of operation with fuel amounts to 12 h.

The experiments went reasonably smoothly, but with some minor irregularities in the circulation of solids between the reactor sections. The outlet gas concentrations during a 2.5 h period of continuous operation are shown in Figure 10.

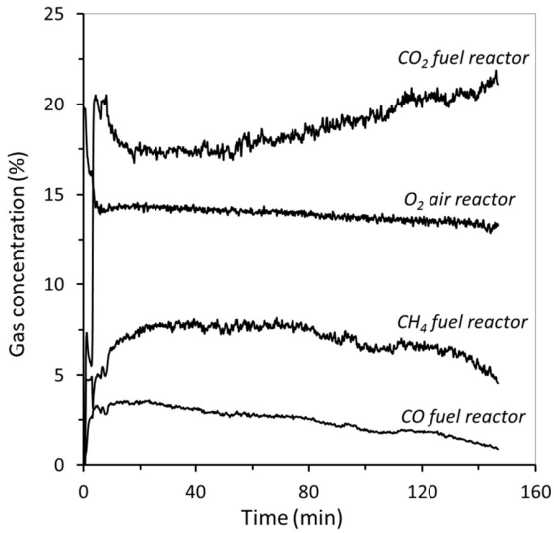

Figure 10. *Outlet concentrations of CO_2, CO and CH_4 from the fuel reactor and outlet concentration of O_2 from the air reactor during continuous operation.*

The conversion of the natural gas was fairly constant during the entire fuel operation campaign. The air flow was varied between 6 L_N/min and 8 L_N/min, but no major effect on the combustion performance could be seen. Operation at a slightly higher temperature (950°C) was attempted but resulted in loss of solids circulation.

This did not result in deactivation of the particles, so when the reactor temperature was reduced back to the initial temperature of 910°C stable operation could once more be established. Loss of solids circulation is typically related to defluidization, a phenomenon that typically is strongly connected to high temperature.

As can be seen in Figure 10, γ_{CH4} was in the order of 60-80%. In general, the improvement in fuel conversion compared to similar experiments using an ilmenite concentrate as oxygen carrier[16] appears to be fairly small.

Particle attrition appears to have been quite moderate with approximately 6 wt% of added materials being collected in various filters downstream the reactor system. There were also some soft agglomerates found in the fuel reactor. These agglomerates could easily be crushed between the finger tips.

4.5. X-ray diffractometry analysis

All fresh samples were examined by X-ray powder diffraction using a Siemens D5000 diffractometer utilizing copper $K\alpha_1$ radiation. Also particles from all successfully conducted experiments were examined. In this case the samples were examined in their oxidized state. The results are summarized in Table 5:

Table 5. Phase composition of oxygen-carriers materials examined in this study (oxidized particles).

Sample	Molar composition	Phases in fresh sample (calcined in air 1100°C)	Phases in used sample (oxidized, from batch reactor)
F17MT51	$(Fe_{0.33}Mn_{0.67})TiO_x$	$(Mn_xFe_{1-x})_3Ti_3O_{10}$	$(Mn_xFe_{1-x})_3Ti_3O_{10}$
F25MT51	$(Fe_{0.50}Mn_{0.50})TiO_x$	$(Mn_xFe_{1-x})_3Ti_3O_{10}$	*See discussion*
F34MT50	$(Fe_{0.67}Mn_{0.33})TiO_x$	$(Mn_xFe_{1-x})_3Ti_3O_{10}$	$(Mn_xFe_{1-x})_3Ti_3O_{10}$
M49T	$MnTiO_x$	$MnTiO_3$	$MnTiO_3$
F31MT9	$(Fe_{0.33}Mn_{0.67})Ti_{0.1}O_x$	$(Mn_x,Fe_{1-x})_2O_3$	$(Mn_x,Fe_{1-x})_2O_3$
F46MT9	$(Fe_{0.50}Mn_{0.50})Ti_{0.1}O_x$	$(Mn_x,Fe_{1-x})_2O_3$	*See discussion*
F61MT9	$(Fe_{0.67}Mn_{0.33})Ti_{0.1}O_x$	$(Mn_x,Fe_{1-x})_2O_3$	$(Mn_x,Fe_{1-x})_2O_3$

Due to the formation of solid solutions it is quite difficult to characterize combined iron and manganese oxides using powder X-ray powder diffraction, but it is possible to draw some conclusions. It seem clear that all fresh ilmenite-pyrophanite analogues consisted of orthorhombic $(Mn_xFe_{1-x})Ti_3O_{10}$, which corresponds to $(Mn_xFe_{1-x})_3O_4+3TiO_2$. While $Fe_3Ti_3O_{10}$ is sometimes found in both fresh and oxidized ilmenite [12], this is probably not the most desired phase for chemical-looping applications. O_2 uncoupling would most likely have been better if further oxidation to the pseudobrookite analogue $(Mn_xFe_{1-x})_2TiO_5+TiO_2$ could have been achieved.

On the contrary, all fresh samples with low Ti content consisted of bixbyite $(Mn_x,Fe_{1-x})_2O_3$, which is the desired and predicted phase. No free titania could be detected in these samples. It seems reasonable to believe that it could be included in the bixbyite structure, but it is also possible that titania could be present in a separate phase but that the low concentrations makes detection by X-ray powder diffraction difficult.

M49T was found to consist of pure pyrophanite $MnTiO_3$. This is actually the intended reduced form, explaining the poor performance of this material. Obviously oxidation of $MnTiO_3$ to higher oxidation states could not be performed at the experimental conditions used in this study. This seemingly disqualifies pyrophanite as oxygen carrier for chemical-looping applications.

Of the used samples, all but two had essentially the same spectra as the fresh ones. The erring ones unfortunately had weak and blurry spectra which were hard to decipher. Used F25MT51 seems to have decomposed into two or more separate phases, possibly $MnTiO_3$, $FeTiO_3$ and $Ti_{0.79}Fe_{1.21}O_3$. F46MT9 seemingly consisted of a combined cubic spinel phase, which was identified (by the software) as $Ti_{0.5}MnFe_{1.5}O_4$. Used F61MT9 also had a few weak and unidentifiable peaks, possibly indicating formation of a new phase besides $(Mn_x,Fe_{1-x})_2O_3$.

5. Conclusions

Seven combined oxide materials based on manganese, iron and titania have been examined as oxygen carrier for chemical-looping combustion with oxygen uncoupling. Particles with different compositions were manufactured by spray drying followed by calcination at 1100°C for 4 h. All fresh materials except pure pyrophanite obtained the desired phase composition, which was $(Mn_xFe_{1-x})_3Ti_3O_{10}$ and $(Mn_x,Fe_{1-x})_2O_3$ solid solutions.

Basic performance was evaluated in a laboratory-scale fluidized-bed reactor at 850-1050°C, in which chemical looping was simulated by switching between oxidizing (5/95% O_2/N_2), inert (100% N_2) and reducing (100% CH_4) conditions. All materials were found capable of releasing minor amounts of gas phase O_2 at relevant conditions. The equilibrium O_2 concentration during fluidization with inert N_2 was up to 0.9%, depending on reactor

temperature and particle composition. Most samples released O_2 at higher concentrations at higher temperatures, but in one case more O_2 was released at intermediate temperature. This is likely an effect of constrained oxidation as function of temperature. As for the reactivity with CH_4, all combined $(Fe_{1-x}Mn_x)Ti_yO_3$ oxides worked quite satisfactory. A CH_4 conversion of 80-99% could be achieved with most of the materials, again with different formulations being favored at different temperature levels. In general, fuel conversion was higher at higher temperatures.

In general, the ilmenite-pyrophanite analogues $(Fe_{0.33}Mn_{0.67})TiO_3$, $(Fe_{0.50}Mn_{0.50})TiO_3$ and $(Fe_{0.67}Mn_{0.33})TiO_3$ performed best at 1050°C, while materials with low titanium content such as $(Fe_{0.33}Mn_{0.67})Ti_{0.1}O_3$, $(Fe_{0.50}Mn_{0.50})Ti_{0.1}O_3$ and $(Fe_{0.67}Mn_{0.33})Ti_{0.1}O_3$ worked better at lower temperature. The latter three all defluidized at 1000°C or above. Pure pyrophanite $MnTiO_3$ released very little gas phase O_2 and hade very poor reactivity with CH_4 and appears to be unsuitable as oxygen carrier.

One material composition $(Fe_{0.50}Mn_{0.50})TiO_3$ was selected and further examined by experiments in a small circulating fluidized-bed reactor using natural gas as fuel. 12 h of operation were recorded and a CH_4 conversion of 60-80% was achieved at 910°C. The overall performance was fairly good, but perhaps not that good considering that similar fuel conversion have been achieved with ilmenite in a quite similar reactor setup[16].

It can be concluded that combined oxides obtained by partially substituting iron for manganese in the ilmenite structure may be feasible as oxygen carrier materials for chemical-looping combustion with oxygen uncoupling. Such materials are capable of releasing gas phase O_2 and appear to have similar mechanical characteristics as ilmenite.

Acknowledgements

This research has received funding from the European Union Seventh Framework Programme (FP7/2007-2013) via grant agreement no° 241401.

References

[1] Intergovernmental Panel on Climate Change. Carbon dioxide Capture and Storage. Cambridge University Press; 2005.
[2] Lewis WK, Gilliland ER. US Patent 2,665,972, 1954.
[3] Richter HJ, Knoche K. Reversibility of combustion processes. ACS symposium series 1983;235:71-85.
[4] Ishida M, Zheng D, Akehata T. Evaluation of a chemical-looping combustion power-generation system by graphic exergy analysis. Energy 1987;12:147-154.
[5] Lyngfelt A, Leckner B, Mattisson T. A fluidized-bed combustion process with inherent CO_2 separation; application of chemical-looping combustion. Chemical Engineering Science 2001;56: 3101-3113.
[6] Mattisson T, Lyngfelt A, Leion H. Chemical-looping with oxygen uncoupling for combustion of solid fuels. International Journal of Greenhouse Gas Control 2009;3:11-19.
[7] Leion H, Mattisson T, Lyngfelt A. Using chemical-looping with oxygen uncoupling (CLOU) for combustion six different of solid fuels. Energy Procedia 2009;1:447-453.
[8] Adanez J, Abad A, Garcia-Labiano F, Gayan P, de Diego LF. Progress in Chemical-Looping Combustion and Reforming technologies. Progress in Energy and Combustion Science 2012;38: 215-282.
[9] Mattisson T. Materials for Chemical-Looping with Oxygen Uncoupling. ISRN Chemical Engineering 2013, Article ID 526375.
[10] Markström P, Linderholm C, Lyngfelt A. Chemical-looping combustion of solid fuels - Design and operation of a 100kW unit with bituminous coal. International Journal of Greenhouse Gas Control 2013;15:150-162.
[11] Corbella BM, Palacios JM. Titania-supported iron oxide as oxygen carrier for chemical-looping combustion of methane. Fuel 2007;86:113-122.
[12] Leion H, Lyngfelt A, Johansson M, Jerndal E, Mattisson T. The use of ilmenite as an oxygen carrier in chemical-looping combustion. Chemical Engineering Research and Design 2008;86:1017-1026.
[13] Adánez J, Cuadrat A, Abad A, Gayán P, de Diego LF, García-Labiano F. Ilmenite activation during consecutive redox cycles in chemical-looping combustion. Energy & Fuels 2010;24:1402-1413.
[14] Cuadrat A, Abad A, García-Labiano F, Gayán P, de Diego LF, Adánez J. The use of ilmenite as oxygen-carrier in a 500W th Chemical-Looping Coal Combustion unit. International Journal of Greenhouse Gas Control 2011;5:1630-1642.
[15] Cuadrat A, Abad A, Adánez J, de Diego LF, García-Labiano F, Gayán P. Behavior of ilmenite as oxygen carrier in chemical-looping combustion. Fuel Processing Technology 2012; 94:101-112.
[16] Rydén M, Johansson M, Cleverstam E, Lyngfelt A, Mattisson T. Ilmenite with addition of NiO as oxygen carrier for chemical-looping combustion. Fuel 2010; 89:3523-3533.

[17] Moldenhauer P, Rydén M, Lyngfelt A. Testing of minerals and industrial by-products as oxygen carriers for chemical-looping combustion in a circulating fluidized-bed 300 W laboratory reactor. Fuel 2012;93:351-363.
[18] Schwebel GL, Leion H, Krumm W. Comparison of natural ilmenites as oxygen carriers in chemical-looping combustion and influence of water gas shift reaction on gas composition. Chemical Engineering Research and Design, 2012;90:1351-1360.
[19] Pröll T, Mayer K, Bolhàr-Nordenkampf J, Kolbitsch P, Mattisson T, Lyngfelt A, Hofbauer H. Natural minerals as oxygen carriers for chemical looping combustion in a dual circulating fluidized bed system. Energ Procedia 2009;1:27-34.
[20] Bidwe AR, Mayer F, Hawthorne C, Charitos C, Schuster A, Scheffknecht G. Use of ilmenite as an oxygen carrier in chemical looping combustion-batch and continuous dual fluidized bed investigation. Energy Procedia 2011;4:433-440.
[21] Azis MM, Jerndal E, Leion H, Mattisson T, Lyngfelt A. On the evaluation of synthetic and natural ilmenite using syngas as fuel in chemical-looping combustion (CLC). Chemical Engineering Research and Design 2010;88:1505-1514.
[22] Berguerand N, Lyngfelt A. Chemical-looping combustion of petroleum coke using ilmenite in a 10 kwth unit-high-temperature operation. Energy & Fuels 2009;23:5257-5268.
[23] den Hoed P, Luckos A. Oxidation and reduction of iron-titanium oxides in chemical looping combustion: A phase-chemical description. Oil and Gas Science and Technology 2011;66:249-263.
[24] Rydén M, Linderholm C, Markström P, Lyngfelt A. Release of gas phase O_2 from ilmenite during chemical-looping combustion experiments. Chemical Engineering and Technology 2012;35:1968-1972.
[25] Azimi G, Rydén M, Leion H, Mattisson T, Lyngfelt A. $(Mn_zFe_{1-z})_yO_x$ combined oxides as oxygen carrier for chemical-looping with oxygen uncoupling. AIChE Journal 2012;59:582-588.
[26] Azimi G, Leion H, Rydén M, Mattisson T, Lyngfelt A. Investigation of different Mn-Fe oxides as oxygen carrier for Chemical-Looping with Oxygen Uncoupling (CLOU). Energy and Fuels 2013;27:367-377.
[27] Rydén M, Leion H, Lyngfelt A, Mattisson T. Combined oxides as oxygen carrier material for chemical-looping combustion with oxygen uncoupling. Proceedings of the 2nd International Conference on Chemical Looping, Darmstadt, Germany, September 2012.
[28] Rydén M, Lyngfelt A, Mattisson T. Combined manganese/iron oxides as oxygen carrier for chemical looping combustion with oxygen uncoupling (CLOU) in a circulating fluidized bed reactor system. Energy Procedia 2011;4:341-348.
[29] Moldenhauer P, Rydén M, Mattisson T, Lyngfelt A. Chemical-looping combustion and chemical-looping with oxygen uncoupling of kerosene with Mn- and Cu-based oxygen carriers in a circulating fluidized-bed 300 W laboratory reactor. Fuel Processing Technology 2012;104:378-389.
[30] Moldenhauer P, Rydén M, Mattisson T, Lyngfelt A. Chemical-looping combustion and chemical-looping reforming of kerosene in a circulating fluidized-bed 300W laboratory reactor. International Journal of Greenhouse Gas Control 2012;9:1-9.
[31] Rydén M, Arjmand M. Continuous hydrogen production via the steam-iron reaction by chemical looping in a circulating fluidized-bed reactor. International Journal of Hydrogen Energy 2012;37:4843-4854.